Six-year Trial of an HV Overhead Line Wide-bodied Composite Insulator

S M Rowland[1,2], I Cotton[1,2], V Peesapati[1], D Chambers[2], C Zachariades[1] and Y Shang[1]

[1] The Dept. of Electrical and Electronic Engineering,
The University of Manchester,
Manchester, M13 9PL, UK

[2] Arago Technology Ltd,
78 Holme Road, Nottingham, NG2 5AD, UK

ABSTRACT

This paper addresses the long-term aging of silicone rubber shedded insulators mounted horizontally, and specifically relates the experience from a highly monitored six-year trial of two composite cross-arms designed for 400 kV. Weather conditions and leakage currents were continuously monitored in this moist and temperate area. In addition, the growth of algae on the surface over time is reported. As expected for the coastal location, strong seasonal variation was seen in leakage currents and this is associated with wind direction and resulting weather variations. Leakage currents remained low but increased linearly with time. Despite apparent large areas of algae growth on upward-facing surfaces, and some associated loss of hydrophobicity on some surfaces, the leakage currents on the insulators continue to be satisfactorily low. Cleaning one of the insulators after five-and-a-half years temporarily returned the current to its original value. In the short-term, leakage currents were heavily dependent on relative humidity, and peak currents are shown to be strongly dependent on the length of preceding periods without precipitation. It is suggested that measurement of these variables may be used to evaluate surface condition and be an effective asset management tool.

Index Terms — **composite insulators, wide-bodied, cross-arm, asset management, silicone rubber, NCI, field trial, leakage current, aging, algae**

1 INTRODUCTION

COMPOSITE insulators are widely deployed in transmission and distribution networks worldwide. From initial installations at lower voltages, these have been used at ever-increasing voltage levels. The predominant use of composite insulators has been as a one-for-one replacement for traditional ceramic insulators. Performance advantages are delivered through hydrophobicity retention, reduced weight, and increased physical robustness. High quality materials, designs and manufacturing processes have commoditized these devices as tension and suspension fittings on overhead lines.

Increasing global demands for electricity, and in particular for low carbon generation, have led to a need to rapidly increase the transmission capacity of existing overhead line infrastructure. In addition, there is an increased expectation that any new lines built optimize the capacity of wayleaves and that designs have reduced visual impact. Traditional composite insulators are designed for tensile strength, and this limits their application in alternative tower designs that provide this power transfer capacity without a corresponding increase in tower size. However, a new generation of composite insulators with compressive strength has provided opportunities for novel compact tower construction.

Manuscript received on 14 February 2020, in final form 22 April 2020, accepted xx Month 20yy. Corresponding author: S. Rowland.

Examples of designs which utilize insulators with compressive strength are plentiful, and can be traced back nearly 50 years [1, 2], with more recent designs being developed to address new needs [3-6]. To provide compressive strength and resistance to buckling, insulator strength elements require large second moment of areas, and are thus wide-bodied structures as opposed to traditional thin-cored composite structures. One design developed by the authors has a novel cross-section, which has the advantage of being solid (not having a hollow core), but minimizes the material used in the pultruded core [7, 8].

There are two key features of high compression strength insulators: Firstly, their core is much wider than that used in traditional tension insulators; secondly, they will often be used in non-vertical orientations. This paper describes a long-term trial of the performance of two composite cross-arms, each comprising four insulators. The trial has allowed investigation into the performance and aging associated with horizontal composite insulators energized in the natural environment over a six-year period. Four of these insulators were of the traditional tension design and four of a wide-bodied compression design.

2 METHODOLOGY

The insulators tested formed two cross-arms. Each cross-arm consisted of two compression insulators and two tension insulators. The tension insulators were sourced commercially and employed high temperature vulcanized, filled silicone rubber, as is standard for that application. The compression members have a cross-section similar to a 'T' shape rather than circular [8], and were fabricated with unfilled liquid silicone rubber sheaths and sheds, which are standard in bushing constructions. Bespoke stress control elements managed the electric fields on the insulators to within standard values (on the surface of the sheath and sheds design-fields were maintained at < 4.5 kV_{rms}/cm, at the sheath termination triple junction < 3.5 kV_{rms}/cm, on metallic end-fittings < 18 kV_{rms}/cm) [9-11]. The assemblies are shown schematically in Figure 1.

The trial site was located 3 km from the coast in the east of Scotland. The cross-arms were installed on a bespoke lattice tower and oriented at 90° from each other (one pointing south, parallel to the coast, and one pointing west, away from the coast). They were installed perpendicular to each other to investigate the impact of orientation on their performance. A dedicated 230 kV single-phase test transformer energized the two cross-arms (voltage to ground of a 400 kV phase-to-phase system). Each of the four insulators comprising each cross-arm were electrically insulated from the tower so that leakage currents to ground could be continually monitored, to an accuracy better than 2%, through independent 20 kΩ resistors. Instrumentation also captured real-time weather conditions on the tower top to enable correlation of electrical behavior with ambient conditions. Solar radiation, rainfall, wind speed and direction, temperature, visibility and relative humidity (RH) were measured. Of the cameras overlooking the cross-arms: One gave a view of one entire cross-arm; another gave a continuous bird's-eye view of a compression insulator's top surface. The latter allowed surface moisture movement to be monitored. The system wirelessly transmitted a summary of data every five minutes for analysis in Manchester. Details of the test site instrumentation are given in [12, 13]. A photograph of the installation is shown in Figure 2, and a plan of the local arrangement in Figure 3. The nomenclature for each insulating member is given in Figure 4.

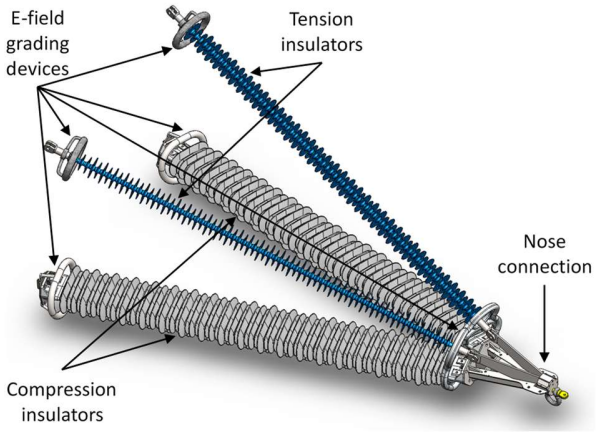

Figure 1. The assembly making up each composite cross-arm.

The cross-arms were 6 m above ground level, and connected to the HV supply by an 8 m long conductor. Details of the two insulator design dimensions are given in Table 1 and cross-

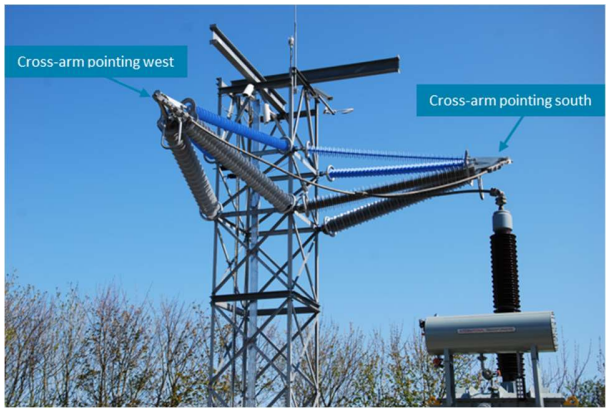

Figure 2. Photograph of the trial site, showing two cross-arms and the high voltage bushing. The cross-arm on the right points due south (along the coastline) and the other points west (away from the coastline).

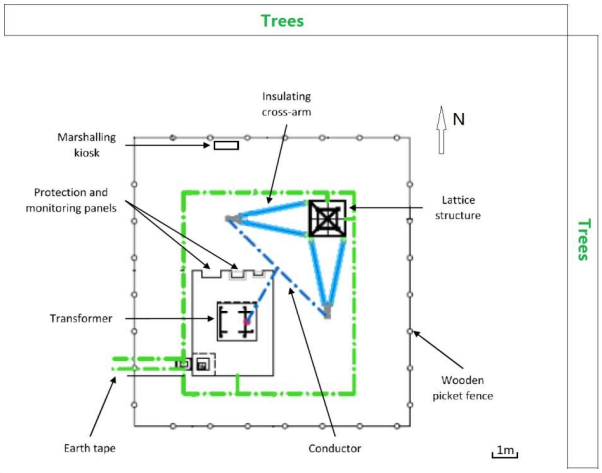

Figure 3. A plan of the site shown in Figure 2. The coastline is to the east of the compound, running north-south.

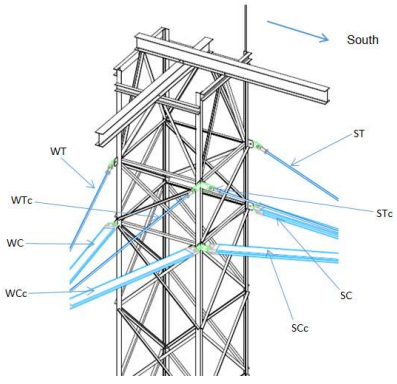

Figure 4. The nomenclature for each insulating member in each cross-arm. The first letter identifies the direction the member points towards (**S**outh or **W**est), the second identifies whether the member is a **C**ompression or **T**ension type. If the element is on the busbar side of the respective cross-arm it is followed by a lower case 'c'.

sections of the wide-bodied insulators are shown in Figure 5. Industry standard creepage and flashover distances were designed into the system with a creepage distance of 12,414 mm and an arcing distance of 3,049 mm for the compression members, and 12,540 mm and 2,960 mm respectively for the tension elements [11]. The compression insulators were turned outwards with sky-facing surfaces angled to the horizontal by a minimum of 6°, so that water flowed off the top surface. The compression insulators were also installed with a length-wise angle to the horizontal of 6° (HV end higher) and the tension insulators at 11° to the horizontal (HV end lower). These angles meet the recommendations of IEC60815 [11]. Wet-flashover performance was verified experimentally in the HV laboratory. The lateral and longitudinal angles of the insulator were chosen to optimize the balance of flashover performance under wet conditions and maintain self-cleaning properties by ensuring water readily ran off the top surfaces.

At the time of installation the trees, identified in Figure 3 around the test area, were well below the height of the cross-arm. Six years later, the trees had grown to be 1 m higher than the cross-arms. This may have had an implication for biological growth on the insulators; an issue reviewed in the discussion.

Table 1. Specification of the tension and compression insulators. For the non-circular insulator, the distance from the edge of the shed to the core sheath surface is given (the projection).

	Tension Insulator	Compression Insulator (Figure 5)
Shed profile	36 small sheds of 160 mm ϕ	39 small sheds of 58.2 mm projection
	35 large sheds of 195 mm ϕ	19 medium sheds of 75.6 mm projection
	Core of 24 mm ϕ	19 large sheds of 90.6 mm projection
Arcing distance	3034 mm	3083 mm
Creepage distance	10297 mm	12470 mm
Creepage Factor	3.39	4.04

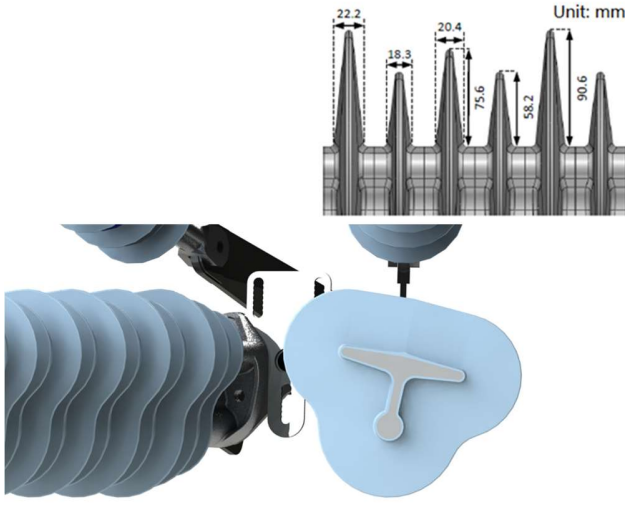

Figure 5. Cross-section of wide-bodied compression insulators (below) and shed design (above) showing the repeat pattern of the insulator.

The site in St Fergus provides a uniquely detailed record of leakage current measurements on both conventional tension insulators and novel wide-bodied insulators designed for 400 kV system application. Weather measurements were taken on the same supporting tower over the six-year period.

3 RESULTS

3.1 LEAKAGE CURRENT

3.1.1 Long-term variation with time

The leakage current is different on each of the eight insulators under dry conditions. This is because of the complex geometry of the assembly. In particular, the spatial relationship between each insulator with the other insulators, the busbar and the lattice tower gives a complex capacitive control of field gradients in each case. The currents measured have been replicated in the laboratory and in FEA analysis and align with expectations. The wide-bodied insulators have greater capacitance and surface conductance, and the insulators closest to the busbar (labeled with an additional 'c' in Figure 4) have a higher capacitance to the HV conductor; these features give rise to higher leakage currents than on their counterparts.

Figure 6 illustrates the variation of leakage current over time. Periods of missing data are due to data/comms failures. There are short-term variations, but a steady rise in current is seen over the six years. The rise is associated with an increase in surface conductivity due to intrinsic aging of the surface, accumulated pollution, or growth of organic matter. In this case, one of the compression elements SCc was washed after 56 months, and for a few months its average current reverted back to original values – confirming it was the organic pollution that increased this current, and the rapid recolonization of the surface by organic matter after cleaning. The increase in daily average leakage current (I_d) is linear in time (t), as shown in Figure 6, and can be represented by:

$$I_d(t) = I_o + K \,.\, t \qquad (1)$$

where values of I_o and K are given in Table 2. I_0 represents the leakage current of each insulator in its location and in pristine condition.

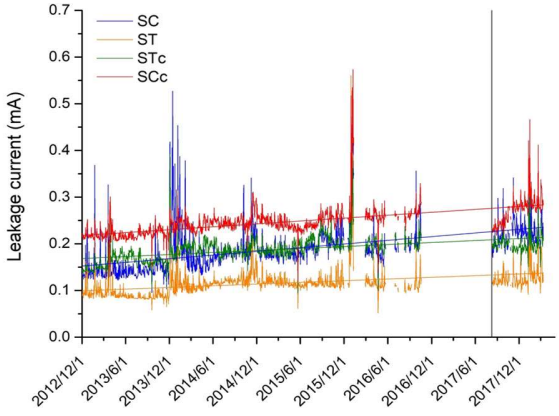

Figure 6. The daily average rms value of current measured on all four of the elements of the south-pointing cross-arm. The missing data in 2017 is due to an outage in instrumentation communications.

Table 2. Measured values of constants for Equation (1).

Insulator	I_o (mA)	K (10^{-3} mA/day)
SC	0.15	0.043
SCc	0.10	0.020
ST	0.17	0.023
STc	0.22	0.034
WC	0.12	0.038
WCc	0.08	0.025
WT	0.22	0.010
WTc	0.22	0.052

3.1.2 Seasonal variation

Within each year there is a clear seasonal variation of leakage current, as would be expected in this north-European coastal climate, summarized in Figure 7. This is due to increased levels of moisture (rain and fog) in winter, and higher temperatures and increased solar radiation intensity and duration in summer. Averaged over all insulators, and taking spring as reference, summer currents are reduced by 5.7%, autumn increased by 5.1% and winter increased by 18.1%. Equation (1) can thus be modified so that:

$$I_d(t) = m\,(I_o + K\,.\,t) \qquad (2)$$

where the leakage current, $I_d(t)$, has a linear time dependence, and also a seasonal dependence, given by the values of m shown in Table 3.

Table 3. Seasonal constants for Equation (2). Other constants are given in Table 2.

	Spring	Summer	Autumn	Winter
Value of '*m*'	1.0	0.94	1.05	1.18

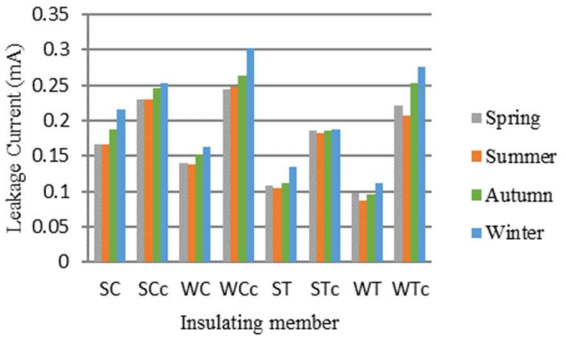

Figure 7. Seasonal variation in leakage currents averaged over three-month periods between 2013 and 2015. A restricted period of three years is compared so that the surface condition is not changed too much within the period considered.

3.1.3 Short-term dependence on relative humidity (RH) and rainfall

Figure 8 illustrates the variation of leakage current on one compression insulator, WC, with wind direction in 2014. Also shown is the leakage current on one insulator over one month with intermittent rain. This illustrates the importance of immediate weather, but also the difficulty in predicting response to rainfall. It is wind direction that controls rainfall in this coastal location; wind from the west, for example, implies no rainfall. The location has a latitude of 57.6° N and so solar radiation is weak, and there is only ~7 hours of daylight at the winter solstice. Nearby Aberdeen has an average monthly rainfall of 41 mm, 11 rain days each month, a monthly

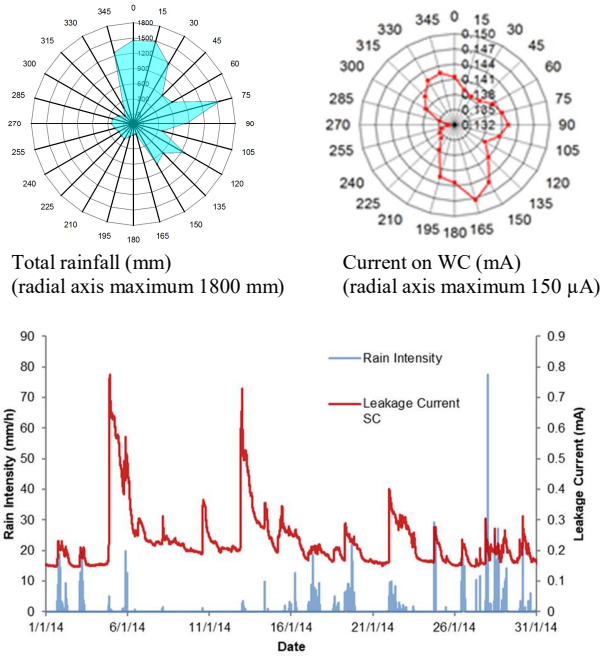

Figure 8. Wind roses showing how rainfall and current on tension member WC varied with wind direction in 2014, and a graph illustrating short-term variation of current and rainfall on SC in January 2014.

maximum average summer temperature of 18°C, and a minimum average temperature of 1°C in the winter [14].

3.1.4 Peak current dependency on the length of periods of dry weather

The most onerous conditions for an insulator leading to highest peak currents are associated with either: Extended periods of surface discharge reducing hydrophobicity, or after long spells without rain during which pollution can accumulate on the insulating surfaces [15, 16]. There is indication that hydrophobicity is compromised in some areas of the insulator due to organic growth (see Section 3.2), and Figure 9 shows a clear dependence of peak current after periods without rainfall on the length of the dry period. The line chosen to fit the data gives the increase in peak current, $I(\tau)$, after a dry period of duration τ by:

$$I(\tau) = \frac{A_\tau}{1+(\tau/\tau_0)^{-p}} \qquad (3)$$

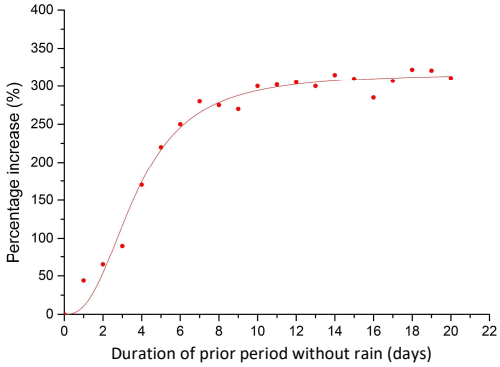

Figure 9. The average percentage increase of the peak current on insulator SC as a function of the duration of the prior period without rain. Data taken from the whole of 2016. The longest dry spell is 20 days. The curve fitted is Equation (3) with A_τ = 317%, τ_0 = 3.7 days, and p = 2.6.

where A_τ is the peak current possible in these circumstances, and p (2.6) and τ_0 (3.7 days) control the shape of the curve.

3.1.5 Peak current dependency on relative humidity

In the absence of rain, relative humidity (RH) is critical in controlling current. Figure 10 illustrates this dependence for one compression and one tension element in the years 2013 and 2017. The lines of best fit given are:

$$I(x) = I_0 + A_1 e^{x/R_1} \quad (4)$$

where $I(x)$ is the leakage current at a given relative humidity, x, and $(I_0 + A_1)$ is the theoretical leakage current when RH is 0%. Constant A_1 reflects the amplitude of the leakage current increase over the range of RH, and R_1 is a measure of the range of values below 100% over which RH is influential. I increases markedly above RH values of $(100 - 3.R_1)$%.

Table 4. Values of parameters for the data in Figure 10, fitted to Equation 4.

Insulator and year	I_0 (mA)	A_1 (mA)	R_1 (%)
SC 2013	0.126	0.50^10^{-4}	14.0
SC 2017	0.163	1.06^10^{-4}	15.0
ST 2013	0.086	0.65^10^{-9}	5.4
ST 2017	0.117	0.32^10^{-10}	4.7

3.2 ORGANIC GROWTH AND HYDROPHOBICITY

3.2.1 Long-term variation with time

After 18 months or so, organic growth became visible in the center of the compression members, but only on the upward-facing surface (Figure 11). Once established, the growth intensified and spread (Figure 12). The undersides of the wide-bodied insulators remained free of organic pollution throughout, presumably because they remained dry. As time passed, the organic growth spread over a wider region of the top surface. However, organic growth never reached the high voltage end, which remained pristine throughout. Figure 13 shows how the algae spread on the top surface in time.

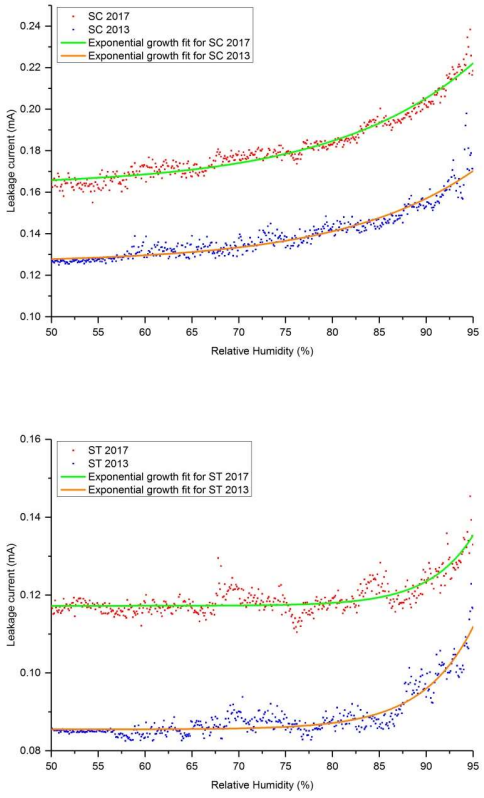

Figure 10. Dependence of leakage current on relative humidity for insulators SC and ST in 2013 and 2017. Parameters for best fit lines are given in Table 4.

Figure 11. Top: Aerial photo of growth of algae in the central region of the compression element SCc after 35 months in service. Bottom left: the run-off of water from the top horizontal surface down the vertical shed led to a spread of algae. Bottom right: The tension insulator STc can be seen to have accumulated algae on the bottom of the sheds, and also to have lost much of its hydrophobicity.

Figure 12. Biological growth after 56 months. Left: on top surface and on sheds of WC insulator. Right: on the WT insulators.

The insulator is designed so that water runs off the top surface. Figures 11 and 12 show that this leads to algae spreading along the drip-lines down the vertical faces of the wide-bodied insulator sheds. It is evident that the tension insulator above the compression element also has algae growing on the shed surfaces, as seen in Figure 11 after 35 months, and Figure 12 after 56 months.

Reductions in the high hydrophobicity associated with silicone rubber sheds are expected over long periods of exposure to light and corona discharges. Experience shows that these changes are not uniform on an insulator's surface, but vary with the local surface orientation and insulator geometry [15, 17, 18]. Layers of organic material have variously been reported but are mainly seen to reduce hydrophobicity [15, 18,

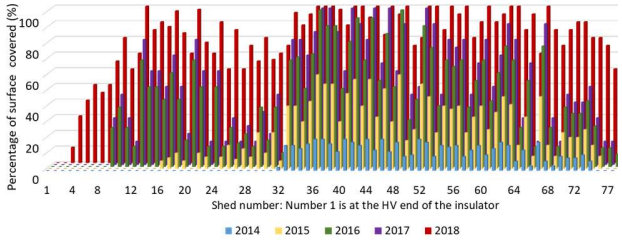

Figure 13. Annual progression of biological coverage of upward-facing surfaces on WC compression insulator up to August 2018, 69 months after installation. Shed 1 is the HV end, with no coverage at any time.

19, 20]. Here, the compression insulators retained their high hydrophobicity levels with the exception of the areas covered with organic material, which saw considerable reductions in hydrophobicity, determined by manual spraying with water and the STRI scale [21].

The photograph of the wet tension element in Figure 11 also illustrates loss of hydrophobicity. The sides of the sheds of the ST insulator that face the sun completely lost hydrophobicity, and on the other side of the sheds, the hydrophobicity was reduced to between HC3 and HC4 on the STRI scale. Loss of hydrophobicity was also seen on WT and WTc. Pollution and algae are seen on these surfaces. The extremities of the lower parts of the insulator sheds can be seen as green in Figure 11.

To investigate how permanent the biological growth effects are, the whole of the south-pointing compression insulator adjacent to the conductor, SCc, was manually cleaned using a soft brush and microfiber cloth. This proved easy to achieve. When the surface was clean to the eye, the newly cleaned areas looked as new and regained hydrophobicity to levels of HC5-6. As reported previously (Figure 6) the leakage currents were also reduced to their original values on reconnection of the supply. However, over the following six months the currents grew back to pre-cleaned levels as the polluted/biological surface conditions were re-established.

3.2.2 Other aging features

Whilst the underside of the wide-bodied insulators remained clean and showed no biological growth, one phenomenon was observed at the high voltage end. This was most pronounced on one of the insulators, but emerged on all the compression elements. This took the form of a thick circumferential line of discoloration on the core between the first two sheds, or between the second and third sheds, as shown in Figure 14. This marking resulted from deposits on the insulator surface which could readily be wiped off, leaving an apparently unblemished surface. We describe this as snake-skin deposits, following the terminology of Peacock and Wheeler who identified circumferential, rather than longitudinal, aging [22] and which one of the authors has previously identified with low-current aging on all-dielectric self-supporting (ADSS) optical cables on high voltage lines [23, 24]. Whilst there is no evidence this region ever got wet in service, manual spraying showed that the core surface immediately around the central line of the snake-skin markings was hydrophobic and the line itself was hydrophilic (HC1-2). This tends to suggest that these markings are caused by low current surface discharges in the high field, and the surface deposits are perhaps pollution from the surrounding rural environment.

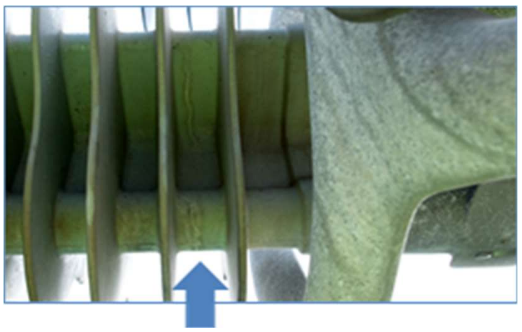

Figure 14. Snake-skin deposits on the underside of a compression member SC in May 2015, after 30 months. This took the form of a line of circumferential discoloration on the core between the first two sheds at the high voltage end, identified with an arrow. The metallic high-voltage stress management fitting is on the right.

5 DISCUSSION

The most notable results from this trial were: The robustness of the composite cross-arms; that the leakage currents remained small throughout (very much less than values associated with dry-band arc formation (~10 mA) or flashover (~100 mA) [15, 16, 23]), and the growth of organic material on the flat upward-facing surfaces. The algae took about three years to emerge, and might have been associated with the growth of nearby trees. A second installation on a rural 132 kV line in Scotland [10], which was not unduly close to trees, showed similar patterns of organic growth. We can therefore draw some clear conclusions, that whilst the local vegetation might have accelerated algae growth here, it will nonetheless occur in other temperate sites.

In contrast to the upward-facing surface, the underside of the compression members remained dry and free of organic material. In addition, water run-off spread the algae from the horizontal faces, where algae tends to grow, down one face of the vertical sheds. Whilst one side of the sheds remained free from contamination, it is an important consideration that half of the potential leakage distance can be considered to be coated with algae. This will directly increase leakage current, and may reduce flashover voltages (but this is yet to be determined). It is also noted, however, that the high voltage end remained free of algae. This is the opposite of the behavior reported on suspension insulators, in which residue was observed only at the high voltage end [18]. The differences in these cases is probably entirely due to the geometry and orientation of the insulators. If the high fields and consequential corona are considered to mitigate against algae growth, it might be supposed that lower voltage systems, or HV systems with improved field management, would suffer algae growth over their entire length. Experience suggests that if insulators are exposed on the ground for long periods before installation, surfaces that are frequently wet become coated with organic material relatively quickly.

No major difference was observed between the south-pointing and west-pointing cross-arms. This is in contrast to [18], in which the side of the insulator facing the direction of sun was seen to have less organic growth and be chemically more damaged. However, the sun is much weaker and seen less frequently in the location considered here compared to that of [18], and the trial reported here was over a shorter period.

Therefore, it is possible that solar radiation will have a more significant impact in the longer term, and this is likely in locations with greater solar intensity. It is noted that regular exposure to the sun also has the benefit of drying wet insulators quickly, thereby inhibiting algae growth. Any short-term differences in performance in this trial due to the orientation of the two cross-arms are dominated by the role of wind direction. Because of the coastal location, the wind direction controls the weather, and the orientation with respect to the sun seems secondary to date.

The role of moisture on the surface of an insulator is critical in developing a resistive current, which adds to the capacitive 'dry' current. This is a complex picture, as illustrated in Figure 8. Laboratory measurements have verified that as the surface becomes conductive, the current magnitude increases and the phase difference to the voltage decreases from ~90°. Whilst most of the eight insulators behave in a similar way in this trial, one of the commercial tension members showed anomalously high peak currents in wet conditions. No reason for this behavior has yet been identified.

Although this site is particularly wet in terms of both rain and fog, Figure 9 and Equation 3 show a clear dependence of peak current observed after periods without rainfall. After dry periods the current increased upon wetting, but the impact did not increase much after nine days without rain. Perhaps longer periods without rain did not further increase the current as a result of the large areas that remained hydrophobic and clean then dominating the impedance of the insulator. It is a feature of the system that the polluted and unpolluted parts of the insulator work in series. It is conceivable that as the insulator ages, this dependence on dry period duration will become more pronounced and the maximum value of current will increase, i.e. the value of A_r, which is the 'saturation current' will increase with age. Perhaps then the important feature of aging is not how poor the worst surface areas are, but rather it is the net area impacted. A change in value of A_r may then be a good indicator of aging and provide a useful asset management tool. A high value of maximum leakage current would clearly be an indicator of aging, but so would a low value of τ_0, which would indicate few dry days are required to accumulate pollution and facilitate the highest values of leakage current on wetting. A high value of p would indicate a greater sensitivity to the duration of the dry period and a quick transition from low to high currents.

Figure 10 shows a very clear and reproducible response to values of relative humidity. Tension members are less responsive to RH than compression members (reflected in lower values of R_1) irrespective of aging, and require a relative humidity of more than 80% to increase leakage current significantly. This may be because the tension members are aging at a slower rate, essentially due to the upward-facing surfaces of the tension members acquiring organic layers faster than the shed surfaces of the horizontal tension members. A key feature is that the response to RH changes as the insulators age. This is quantifed in Table 4: The absolute and relative changes in leakage current are seen to have increased in the aged insulators. The values of both I_0 and A_1 are seen to increase for both the tension and compression insulators. This too may then lend itself to being a tool for asset condition monitoring.

The snake-skin markings on the underside of the compression members in the high voltage region are thought to be the accumulation of dirt from the agricultural environment. It is unclear whether this is related directly to the nature of the more permanent damage witnessed on ADSS cables, but the general picture of very low currents creating this pattern of activity is similar [24]. This does not appear to be a threat to the insulators, which comprise materials superior in discharge resistance to those used in ADSS cables (silicone rubber-based compared with polyolefin-based). However, the development of this process should be examined carefully in the future, and may be mitigated by improved stress control.

4 CONCLUSIONS

The site in St Fergus has given a uniquely detailed record of six years' leakage current measurements, both on novel wide-bodied insulators and conventional tension insulators designed for a 400 kV system. In addition, weather measurements have been taken on the same supporting tower in real time. It is not surprising in this location that the instrumentation and communications systems are less reliable than the high voltage installation. However, this is a salutary lesson for long-term asset health monitoring in the field.

Significant organic growth has been seen to develop on both tension and compression elements, however the upward-facing surfaces of the compression elements saw the fastest growth. The growth started in the center of the insulators' lengths and worked outwards, but did not reach the HV end, which seems protected by the high fields and associated ozone in that area. The shape and slope of the top surface of the insulator core is a key factor in algae formation and subsequent propagation over sheds through water run-off.

The undersides of the wide-bodied insulators, which remain dry, do not develop organic growth, but a secondary effect leading to non-permanent marks on the cable surface, termed snake-skin markings, is thought to be associated with low-level currents. These marks are believed to result from accumulation of small environmental dirt particles.

Average leakage current is seen to increase linearly with time on all the insulators over the trial period, but remains at low levels. There is a clear dependence on ambient relative humidity and it is proposed that the magnitude of the variation of leakage current with RH may be used as an indicator of asset health. Similarly there is a strong correlation of the peak current after rainfall with the duration of preceding dry periods. It is suggested that this might also be a sensitive asset management tool to assess surface condition. Measuring leakage current, RH and rainfall have an advantage over trying to directly determine surface condition in that sampling of materials is not needed locally. However, knowledge of very local weather conditions is required in both these cases. In particular, seasonal variation in leakage current is substantial – requiring long periods of monitoring to yield reliable information.

It has been shown that remote monitoring of leakage currents in wet and dry conditions can be used to give some information concerning asset health. In practice this might be accompanied by visual inspection in some cases, which would be readily achieved given that only exposed surfaces grow algae. Results here suggest that although the algae can readily be removed,

subsequently the surface returns to its polluted condition over several months. More work is required to optimize proactive maintenance procedures based on an asset management framework such as proposed in [25].

ACKNOWLEDGMENT

The authors acknowledge the support of Scottish and Southern Energy Power Distribution and National Grid. Many people contributed to making this trial a reality: Special thanks to Alistair MacLeod, John Baker and Martin Queen.

REFERENCES

[1] I. Kimoto, K. Kito, and K. Ueno, "Insulator cross-arms for 345-kV EHV transmission line," IEEE Trans. Power App. Sys., vol. 90, pp. 756-764, 1971.
[2] B. St. C. Gibson, "Comments on 'Insulator cross-arms for 345-kV EHV transmission line," IEEE Trans. Power App. Sys., vol. 90, pp. 765-766, 1971.
[3] Bystrup, "the T-Pylon," 2014. https://www.powerpylons.com/t-pylon.
[4] Y. Gao *et al*, "Electric field and electromagnetic environment analyses of a 500 kV composite cross arm," *Annu. Rep. Conf. Electr. Insu. Dielectr. Phenom. (CEIDP),* 2015, pp. 399–402.
[5] B. Burkhardt *et al,* "New solutions with composite insulators and composite structures for compact lines," *Int. Conf. Electricity Distribution (CIRED), 2003,* paper 54.
[6] J. F. Goffinet, I. Gutman, and P. Sidenvall, "Innovative insulated cross-arm: Requirements, testing and construction," *12th Int. Conf. Live Line Maintenance (ICOLIM)*, 2017.
[7] S. M. Rowland *et al*, "Development of insulating cross-arms for compact HV lattice tower structures," *CIGRE,* 2014, B2-107.
[8] I. Cotton *et al,* "Support Towers, Insulating Cross-arms and Insulating Members for High Voltage Power Networks," 2011.
[9] V. Peesapati *et al*, "3D Electric Field Computation of a Composite Cross-Arm*," IEEE Int. Symp. Electr. Insul. (ISEI),* 2012.
[10] C. Zachariades *et al*, "Development of Electric Field Stress Control Devices for a 132 kV Insulating Cross-arm using Finite Element Analysis," IEEE Trans. Power Del., vol. 31, Iss. 5, pp. 2105 – 2113, 2016.
[11] Selection and dimensioning of high-voltage insulators intended for use in polluted conditions - Part 3: Polymer insulators for a.c. systems, IEC TS 60815 -3.
[12] C. Zachariades *et al*, "A Coastal Trial Facility for High Voltage Composite Cross-arms," *IEEE Int. Symp. Electr. Insul. (ISEI),* 2012, pp. 78-82.
[13] C. Zachariades, S. M. Rowland, and I. Cotton, "Real-time monitoring of leakage current on insulating cross-arms in relation to local weather conditions," *IEEE Electr. Insul. Conf. (EIC),* 2013 pp. 397-401.
[14] https://www.timeanddate.com/weather/uk/aberdeen/climate, Accessed 26th October 2019.
[15] M. A. R. M. Fernando and S. M. Gubanski, "Ageing of silicone rubber insulators in coastal and inland tropical environment," IEEE Trans. Dielectr. Electr. Insul., vol. 17, Iss. 2, pp. 326-333, 2010.
[16] I. Ramirez, R. Hernandez, and G. Montoya, "Measurement of leakage current for monitoring the performance of outdoor insulators in polluted environments," IEEE Electr. Insul. Mag., vol. 28, Iss. 4, pp. 29-34, 2012.
[17] Y. Xiong, S. M. Rowland, J. Robertson, and R. J. Day, "Surface analysis of asymmetrically aged 400 kV silicone rubber composite insulators," IEEE Trans. Dielectr. Electr. Insul., vol. 15, Iss. 3, pp. 763-770, 2008.
[18] S. M. Rowland, J. Robertson, Y. Xiong, and R. J. Day, "Electrical and material characterization of field-aged 400 kV silicone rubber composite insulators," IEEE Trans. Dielectr. Electr. Insul., vol. 17, Iss. 2, pp .373-383, 2010.
[19] S. Kumagai, "Influence of Algal Fouling on Hydrophobicity and Leakage Current on Silicone Rubber," IEEE Trans. Dielectr. Electr. Insul., vol. 14, Iss. 5, pp. 1201-1206, 2007.
[20] S. Yang, Z. Jia, and X. Ouyang, "Effects of algae contamination on the hydrophobicity of high-voltage composite insulators," High Voltage, vol. 4, Iss. 3, pp. 234-240, 2019.
[21] Hydrophobicity Classification Guide, STRI Guide 92/1, 1992.
[22] A.J. Peacock and J.C.G. Wheeler "Development of aerial fibre optic cables for operation on 400 kV power lines," IEE Proc. Science, Measurement and Technology, vol. 139, Iss. 6, pp. 304 – 314, 1992.
[23] S. M. Rowland and F. Easthope, "Electrical Ageing and Testing of Dielectric Self-Supporting Cables for Overhead Power Lines," Proc IEE Part A, vol. 140, pp. 351-356, 1993.
[24] S. M. Rowland, K. Kopsidas, and X. Zhang, "Ageing of Polyethylene ADSS Sheath By Low Currents," IEEE Trans. Power Del., vol. 25, Iss. 2, pp. 947-952, 2010.
[25] A. Tzimas *et al*, "Asset Management Frameworks for Outdoor Composite Insulators" IEEE Trans. Dielectr. Electr. Insul,, vol. 19, Iss. 6, pp. 2044-2054, 2012.

Simon Rowland (F '14) completed a BSc in physics at The University of East Anglia and his PhD at Chelsea College, London University. He worked for many years on dielectrics and their applications in multinational companies prior to joining The Dept. of Electrical and Electronic Engineering in The University of Manchester in 2003. He was appointed Professor of Electrical Materials in 2009, and Head of Dept. from 2015-19. He was President of the IEEE Dielectric and Electrical Insulation Society 2011-12.

Ian Cotton received a B.Eng. in electrical engineering from The University of Sheffield, U.K. in 1995 and a Ph.D. from The University of Manchester Institute of Technology (UMIST) in 1998. He is Professor of High Voltage Technology at The University of Manchester and the Director of Manchester Energy. His main research interests include power systems transients, the use of higher voltage systems in aerospace applications and power system induced corrosion.

Vidyadhar Peesapati received a degree in electrical and electronics engineering from The University of Madras in 2001, and both an MSc in electrical power engineering in 2006 and a PhD in 2010 from The University of Manchester. He is currently a Research Fellow in the Dept. of Electrical and Electronic Engineering, The University of Manchester. His main research interests include condition monitoring techniques and asset management. Dr. Peesapati is a Chartered Engineer and a member of The IET.

David Chambers graduated from The University of Nottingham in Materials Science. He spent 10 years as an engineer and senior manager in EPL Composites developing innovative products for a wide range of markets. He is now Managing Director of Arago Technology. He also is a Director of Innovation to Industry (I2I), an engineering company that specializes in all aspects of the innovation process.

Christos Zachariades received a B.Eng. in electrical and electronic engineering in 2009, an MSc in electrical power systems engineering in 2010, and a PhD in electrical and electronic engineering in 2014 from The University of Manchester. He is currently a lecturer in Electrical Energy with The University of Liverpool. Dr. Zachariades is a Chartered Engineer and a member of The Institution of Engineering and Technology.

Yingqiang Shang received a B.Sc. in electrical and automation engineering from North China Electric Power University, the M.Sc. in Electrical Energy Systems from Cardiff University, and a Ph.D. in from the University of Manchester. His research interests include composite insulators, leakage current measurement, finite element analysis and status assessment. He is now working at Beijing Power Cable Company, State Grid, China.